# EduceLab Herculaneum Scroll Data (2023) Info Sheet

C. Seth Parker, Stephen Parsons

## 1. Introduction

This document describes the Herculaneum data captured at the Diamond Light Source (DLS) I12 beamline from Sept. 30 to Oct. 3, 2023. This includes information about the samples and what to expect in the scan volumes, along with additional information: how they were fixtured for scanning, acquisition methods, and the reconstruction protocol. The beginning sections of the document describe the general methodology which was applied to all samples. These are followed by scan-specific sections which describe any variances between scans.

This is a living document which will be updated as new reconstructions are released. Please refer to the document version number and date in the footer to identify which version of the document that you are reading.

## 2. Samples

All samples are from the Officina dei Papiri Ercolanesi, Biblioteca Nazionale di Napoli Vittorio Emanuele III in Naples, IT. All samples were hand-carried to the DLS by a representative of the Officina. Samples are divided into two categories: fragments and intact scroll parts.

Fragments are detached pieces from those scrolls which have been physically opened. Fragments show visible text on their surfaces. Fragment scans are primarily intended to be used as training data for ink detection methods.

Intact scroll parts are still-rolled parts of scrolls which do not show visible text on their surfaces. Intact scroll scans are primarily intended to be used as prediction data for recovering yet unseen text. Due to prior physical intervention and/or damage, intact scroll parts may or may not represent an entire scroll. All intact scroll parts in this acquisition session are each a *midollo*[1] (translation: marrow) of a larger scroll – the cylindrical interior of a scroll left still rolled after the physical unwrapping of outer wraps (or the *scorza,* translation: bark).

[1] Janko, R. (2016). *How to Read and Reconstruct a Herculaneum Papyrus*. Ars Edendi, 117. Stockholm University Press.

## 2.1. PHerc 332

*Figure 2-1: Photograph of PHerc 332.*

PHerc 332 is an intact scroll part with approximate diameter 26 mm and length 77 mm.

## 2.2. PHerc 1667

*Figure 2-2: Photograph of PHerc 1667.*

PHerc 1667 is an intact scroll part with approximate diameter 30 mm and length 85 mm.

## 2.3. PHerc 1667, Cr. 1, Fr. 3

*Figure 2-3: Photograph of PHerc 1667, Cr. 1, Fr. 3.*

PHerc 1667, Cr. 1, Fr. 3 is a fragment from the unrolling efforts of PHerc 1667 (above). The fragment measures approximately 14 x 23 mm. This was chosen for imaging as it is a very rare example of suitable fragment and intact scroll part from the same original scroll (most likely). The physical unrolling efforts result in many cornici (trays) of many fragments each, so the naming means: Papyrus Herculaneum 1667, cornice (tray) 1, fragment 3.

## 2.4. PHerc 51, Cr. 4, Fr. 48

*Figure 2-4: Photograph of PHerc 51, Cr. 4, Fr. 48.*

PHerc 51, Cr. 4, Fr. 48 (approximately 19 x 28 mm) was selected for its combination of clear text, clean surface, sturdy construction, and ideal size for imaging.

# 3. Fixturing

Fixturing is the process of placing samples in support structures (cases, frames, etc.) so that the sample can then be safely mounted in the CT scanner. With a few exceptions (which will be noted), once a sample was mounted in the I12 experimental hutch, it was not unmounted until all scans of that sample were acquired.

## 3.1. Intact scroll parts

Full 3D models of each intact scroll part were captured using photogrammetry in the summer of 2023. These 3D models were used to design cylindrical, form-fitting scan cases which would support the samples in an upright orientation during scanning. To accommodate fixturing samples of such a small size, a tolerance of 3 mm was included on all sides of the sample in the case design. Please refer to the accompanying Fixturing References documents to see 3D renders of the scan cases and the expected orientation of the samples within the cases. The cases were 3D printed from Nylon 12 using HP Multi Jet Fusion.

The intact scroll parts were placed in their cases prior to the imaging session by the conservators in the Officina dei Papiri Ercolanesi. To protect the samples from damage caused by abrasion, Teflon Relic Wrap was placed in the lining of the case to create a barrier between the case and the sample. The two halves of the cases were held together during transport and scanning by rubber bands. Once mounted, the intact scroll parts were not removed from their scan cases until they were returned to the Officina dei Papiri Ercolanesi at the conclusion of the scan session. Renders of the cases and scrolls are shown below.

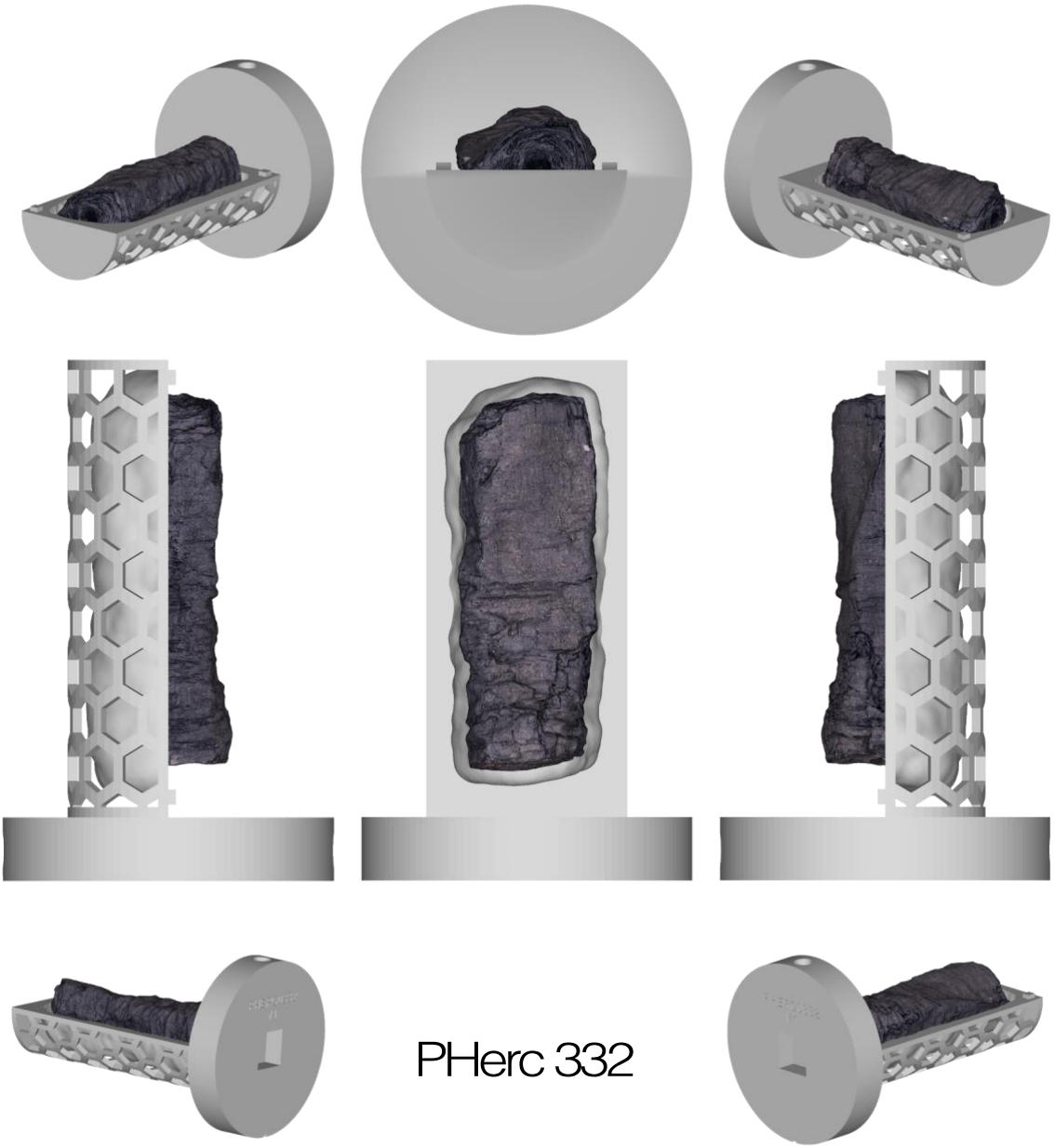


*Figure 3-1: Reference renders for PHerc 332 showing the expected orientation of the sample with respect to the case.*


*Figure 3-2: Reference renders for PHerc 1667 showing the expected orientation of the sample with respect to the case.*

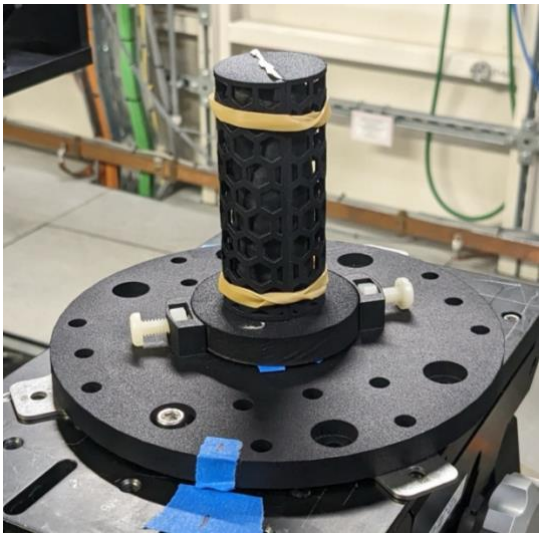

*Figure 3-3: PHerc 332 in its scan case, mounted on the I12 sample stage.*

Mounting the cases to the I12 sample stage followed a similar protocol to that used in previous scan sessions. A universal base plate was first mounted to the I12 sample stage. The scan case was then placed on the base plate such that notches in both parts align in an expected orientation. Nylon bolts were then used as set screws to secure the scan case to the base plate. Due to the small size of the intact samples in this experiment, 2 mm metal shims were placed between the sample stage and the base plate to ensure the bottom of the samples was entirely in the field-of-view.

### 3.1.1. Glass beads

During the first scan of PHerc1667, we noticed relatively dense spheroids on the exterior of the scan case. These spheres were often concentrated in narrow cavities, such as in the joins where the honeycombed cylinder meets the outer wall of the lining.

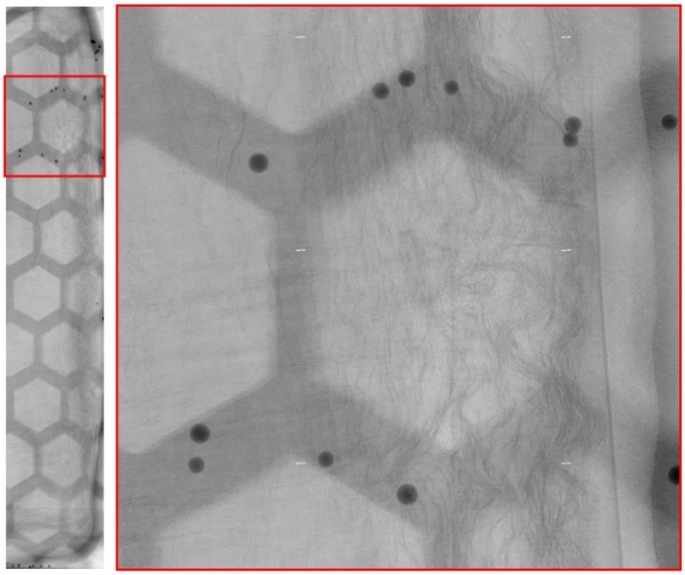

*Figure 3-4: Glass beads as seen in x-ray projection images of PHerc 1667.*

We inspected the PHerc332 case and found small, white beads in similarly narrow regions of that case's exterior. Using a small pick, we removed as many of these beads as possible from the PHerc332 scan case. Not wishing to disturb the placement of PHerc1667, we did not remove any beads from that case.

Since the beads have significantly higher x-ray attenuation than the samples, there are minor streaking artifacts in those slices of which include beads. Given the placement of the beads on the exterior of the case, as opposed to being directly adjacent to the sample, we do not anticipate that these artifacts will introduce significant issues during data analysis.

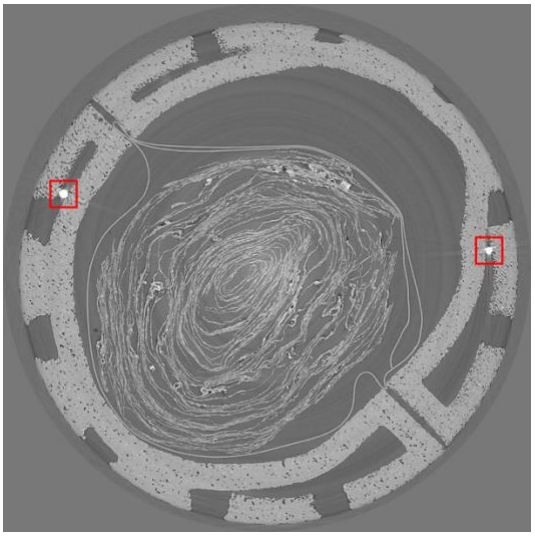

*Figure 3-5: Example slice from PHerc 1667 (53keV, 7.91um) showing two beads on the exterior of the scan case.*

We hypothesize that these are glass beads used to smooth and finish the 3D prints, and that they had simply gotten stuck in the narrowest spaces of the cases. EDS analysis on three of the removed beads shows the presence of C, O, Al, Si, and P.

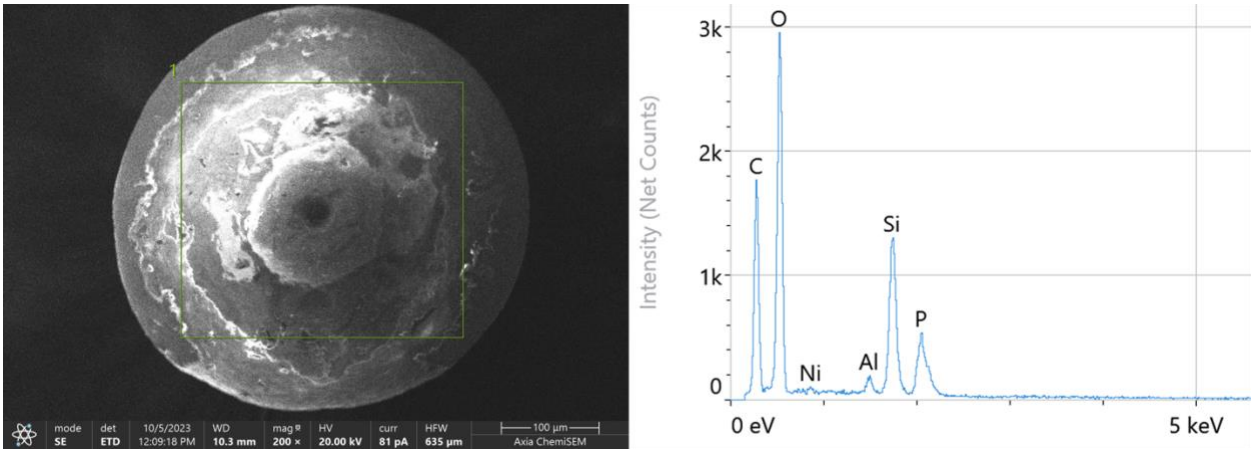


*Figure 3-6: EDS analysis of one of the beads removed from the scan case for PHerc 332. Images courtesy Dr. Michael Detisch (University of Kentucky)*

### 3.2. Fragments

The fragments are already adhered to a backing sheet of conservation rice paper as a result of their original conservation. For scanning, this piece of rice paper is sandwiched between frames laser cut from conservation mat board. The backing piece is rectangular, and a top piece is similar but with a rectangular hole cut to expose the fragment. This stack is clamped together, and the assembly is fixtured into the I12 sample stage for imaging.

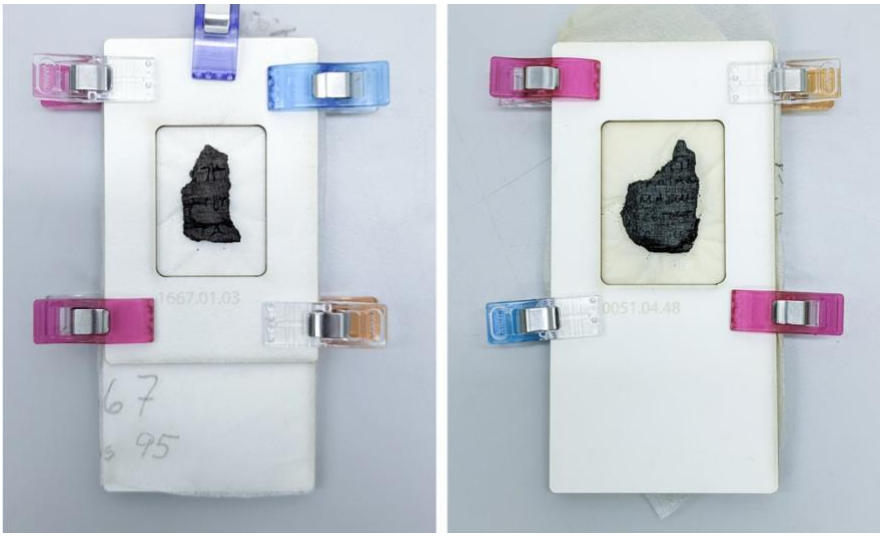

*Figure 3-7: PHerc 1667, Cr. 1, Fr. 3 (left) and PHerc 51, Cr. 4, Fr. 48 (right) fixtured for scanning.*

## 4. Acquisition

All samples were imaged multiple times, and scans were primarily differentiated by effective detector pixel size and incident energy. Due to the limited field-of-view of the imaging system, we employed a half-acquisition, grid scanning technique of multiple overlapping CT acquisitions to capture complete x-ray projection datasets for each sample.

### 4.1. Pixel size

The beamline provides four optical modules for its high-resolution imaging camera[2]. We exclusively used I12 optical modules 2 and 3 which have isotropic pixel sizes of 7.91 um and 3.24 um, respectively.

### 4.2. Incident energy

The monochromatic beam at the I12 beamline is filtered from a white beam[3] using an Si (111) monochromator. The resulting monochromatic beam has an incident energy range of 53-150 keV, and the incident energy used during a particular scan is selected by tuning the crystals of the monochromator. It is worth noting that the reported incident energy for all scans is the

[2] See “High resolution imaging camera”: https://www.diamond.ac.uk/Instruments/Imaging-and-Microscopy/I12/Detectors-at-I12.html

[3] The flux of the white beam is high enough that it poses physical risk to delicate samples, thus the lower flux monochromatic beam was used for these experiments.

*nominal* incident energy. The design of the monochromator is such that the actual incident energy of the x-rays reaching the sample may vary by a few keV from the reported energy value.

### 4.3. Grid scanning

The fixed fields-of-view of the optical modules used for our scans were significantly smaller than the sizes of most of our samples: 20 mm x 12 mm for optical module 2 and 8 mm x 7 mm for optical module 3. As such, no scan could capture an entire sample in a single field-of-view. To capture complete datasets at all our target pixel sizes, we employed grid scanning, a commonly used technique for extending the effective field-of-view of a tomographic system.

Grid scanning works by capturing multiple, partially overlapping CT scans of a sample, and then stitching the resulting x-ray projection data during reconstruction to produce larger projections (or sinograms) than were captured at scan time. To ensure full coverage of the sample, the sample is translated horizontally and vertically with respect to the axes of the detector between each individual CT scan. Thus, the individual scans are captured in a 2D grid pattern where grid rows traverse the vertical axis of the sample (the axis parallel to the axis of rotation) and grid columns traverse the horizontal axis. By adding more grid columns, you increase the field-of-view of each individual tomographic slice. By adding more grid rows, you increase the number of slices in the volume. The instrumentation at I12 makes it possible to automate the acquisition of grid scans for full samples by simply providing a few simple parameters: grid shape, grid offsets, exposure time, and rotational step size.

Each grid cell in a grid scan is functionally a standalone CT dataset. At the start of each grid cell, the sample was moved out of the field-of-view and 100 flatfield and 100 dark field images were captured. The sample was then returned to the field-of-view using the appropriate translational offsets for the given grid cell. Once in place, the sample was continuously rotated over 360 degrees and images were captured at regular rotational intervals. For this scan session, a rotational interval of 0.05 degrees was used for all scans.

## 5. Reconstruction

Prior to reconstruction, the projection images within each grid row are horizontally stitched together. This row is then reconstructed using filtered backprojection (FBP), resulting in a set of reconstructed CT slices through that row. The FBP reconstruction process is itself a multi-step pipeline with various filters and stages. More information is forthcoming.

These rows overlap vertically. Those overlaps are detected, and the rows are stitched together post-reconstruction, resulting in a single merged volume for the sample. The movement stages utilized to translate the sample between row acquisitions are precise enough that the overlap point between scan rows tends to be within a ~ 3 slice window, or ~ 10 um. Hardcoding the overlap point between rows would save some time and would likely have a negligible impact on the resulting data quality, but the overlaps are still computed as a form of quality control to ensure the detected overlaps are in the expected range. This confirms the acquisition went as planned. To find the overlap point, slice 0 of the next row is compared against a set of slices

from a search window in the first row. The correlation between candidate slices and the next row is computed, and the highest correlating slice is identified as the overlap point. The script also verifies that, within the search window, the correlation is monotonic increasing before the overlap point and monotonic decreasing afterwards. This is just another sanity check, confirming that the search window spans the actual overlap point and not another region entirely (in which case the correlation would not peak so cleanly).

The output of reconstruction is a float32 merged 3D volume of the dataset. This will be provided, broken into 1000-slice .hdf slabs to achieve reasonable file sizes. The float values are the raw outputs of the reconstruction process and tend to have small values (e.g. ranging in one dataset from -0.000103 to 0.000265).

A Volume Cartographer-ready .volpkg volume of 16-bit unsigned integer .tif slices will also be provided. The raw float values from reconstruction are windowed to [0, (2^16 – 1)] using the 0.01 and 99.99 percentile values sampled from the full volume to remove outliers.

## 6. Working across volumes

Each sample was imaged multiple times, to capture a range of incident energies and pixel sizes. This results in multiple datasets, or multiple volumes, per sample. The scanning and reconstruction protocols are designed to enable the alignment, or registration, of these volumes. This way, segmentations performed in one volume can be applied without duplicated effort to the other volumes of the same sample.

To achieve this, a “canonical” dataset will be defined for each sample. This volume should be used for initial segmentation efforts.

Volume Cartographer now supports volume-to-volume transforms (additional info) to align additional scans to the canonical scans. For additional scans of an object, we compute the affine transform from that scan to the canonical scan. It is stored in `transforms/` in the `.volpkg`. You can use a segmentation from the canonical volume to render texture images or surface volumes from other volumes in VC simply by specifying --volume in the VC command. It will find the transform and apply it to the mesh before sampling the target volume. The idea is that a single segmentation can be applied to all scans of that object, so the data in the segments can be compared directly. Check out the above links for more information and let us know if you have any issues!

Volume slice ordering follows this spatial convention: slice 0 is physically at the bottom of the sample, and increasing slice indices move up the sample. This convention is used for both fragments and intact scroll parts. As the orientation of the text for the intact scroll parts was not known prior to the scan, slice 0 will correspond to the bottom of the sample as scanned, but this may or may not represent the bottom of the text within the sample. Please refer to the accompanying Fixturing References documents to see 3D renders of the scan cases and the expected orientation of the samples within the cases.

Note: Due to differences in the processing pipeline, this convention is followed in the 2019 fragment scans (the Kaggle fragments), but not for the intact scrolls (scroll 1 and scroll 2), for which the lower-numbered slices are physically higher on the sample as mounted. Scroll 1 and scroll 2 should be the only departures from this convention.

## 7. Datasets

| Sample | 53 keV, 7.91 um | 53 keV, 3.24 um | 70 keV, 7.91 um | 70 keV, 3.24 um | 88 keV, 7.91 um | 88 keV, 3.24 um | 90 keV, 7.91 um | 90 keV, 3.24 um | 105 keV, 7.91 um | 105 keV, 3.24 um |
|---|---|---|---|---|---|---|---|---|---|---|
| PHerc 332 | | **Canonical** | | | | | | | | |
| PHerc 1667 | | | | | | **Canonical** | | | | |
| PHerc 1667 Cr 1 Fr 3 | | | | **Canonical** | | | | | | |
| PHerc 51 Cr 4 Fr 8 | | **Canonical** | | | | | | | | |

New! Released Coming soon N/A

### 7.1. PHerc 332, 53 keV, 3.24 um (canonical)
Volume

### 7.2. PHerc 332, 53 keV, 7.91 um
Volume, transform

### 7.3. PHerc 332, 70 keV, 3.24 um
Volume, transform

### 7.4. PHerc 1667, 88 keV, 3.24 um (canonical)
Volume
Bright beads around the scroll case: see Section 3.1.1.

### 7.5. PHerc 1667, 53 keV, 7.91 um
Volume, transform

### 7.6. PHerc 1667, Cr. 1, Fr. 3, 70 keV, 3.24 um (canonical)
Volume

### 7.7. PHerc 1667, Cr. 1, Fr. 3, 70 keV, 7.91 um
Volume, transform

### 7.8. PHerc 51, Cr. 4, Fr. 8, 53 keV, 3.24 um (canonical)
Volume

### 7.9. PHerc 51, Cr. 4, Fr. 8, 53 keV, 7.91 um

Volume, transform

### 7.10. PHerc 51, Cr. 4, Fr. 8, 70 keV, 3.24 um

Volume, transform

### 7.11. PHerc 51, Cr. 4, Fr. 8, 88 keV, 3.24 um

Volume, transform